Coupled thermo-structural analysis of a bimetallic strip using the absolute nodal coordinate formulation

Gregor Čepon, Blaž Starc, Blaž Zupančič, Miha Boltežar

May 16, 2017

Cite as:
Gregor Čepon, Blaž Starc, Blaž Zupančič and Miha Boltežar. Coupled thermo-structural analysis of a bimetallic strip using the absolute nodal coordinate formulation. Multibody System Dynamics. In Press. Accepted manuscript, available online: 16-MAY-2017
DOI: 10.1007/s11044-017-9574-7

Abstract

A bimetallic strip consists of two different metal pieces that are bonded together. Due to the different coefficients of thermal expansion, exposing the strip to temperature induces thermal stresses that cause the structure to bend. Most often, incremental finite-element methods that introduce element nodal coordinates have been successfully applied to analyze the thermally induced vibrations in such systems. The exposure of these bimetallic strips to high temperatures results in large deflections and deformations, where the effects of the rigid-body motion and large rotations must be taken into account. For classic, non-isoparametric elements such as beams and plates the incremental methods do not result in zero strains under arbitrary, rigid-body motion. Therefore, in this paper a new model of a bimetallic-strip is proposed based on a coupled thermo-structural analysis using the absolute nodal coordinate formulation. The applied, non-incremental, absolute nodal coordinate formulation uses a set of global displacements and slopes so that the beam and the plate elements can be treated as isoparametric elements. In order to simulate the bimetallic strip's dynamic response, the formulation of the shear-deformable beam element had to be extended with thermally induced stresses. This made it possible to model the coupled thermo-structural problem and to represent the connectivity constraints at the interface between the two strips of metal. The proposed formulation was verified by comparing the responses using a general-purpose finite-element software.

1 Introduction

Bimetallic strips are used in various engineering applications, such as thermometers, thermostats, miniature circuit breakers, etc [1–4]. Most bimetallic systems are constructed by bonding together two strips with different coefficients of thermal expansion. When heated, the so-called active component expands more than the passive one, causing the bimetallic strip to bend. This effect is mainly used for the fabrication of temperature-controlled, residual-current circuit breakers with overcurrent protection. The triggering function is performed by a bimetallic plate element, which has to deform within a given time to generate a force and trigger the switching mechanism. Recently, thermally activated bimetallic microbeams have been the mainstays of MEMS technology [5]. As electrothermal bimetal actuators have the advantage of a large force and displacement under a low driving voltage [6], they have been effectively applied to micromachined valves and pumps [7].

The first model of the bimetallic beam was developed by Timoshenko [8]. The models presented in [9–11] are extensions of the Timoshenko model and propose a uniform temperature distribution and loading during the stress-strain calculation. In the classic handbook [12] the beam-theory solution for the deflections and stresses of a bimetallic strip is presented. Since 1960 many investigators applied numerical, mainly finite-element, methods to analyze the thermally induced vibrations of bimetallic structures. Usually, bimetallic strips are subjected to high temperatures that result in large displacements and deformations [1]. Moreover, due to their high operating speeds the effects of the inertial forces must be taken into account. Therefore, the aim in the field is to present an efficient and reliable formulation to model the dynamic responses of such systems. Several finite-element formulations have been proposed for the large displacement and deformation of flexible bodies. Incremental finite-element formulations that introduce element nodal coordinates have been successfully applied for large-deformation analyses. It is important to note that for non-isoparametric elements such as beams and plates the incremental methods do not result in zero strains under arbitrary rigid-body motion. To overcome this problem Shabana [13] proposed a non-incremental, absolute nodal coordinate formulation (ANCF) where the set of coordinates consists of global displacements and slopes [14–16]. Using this set of coordinates the beam and plate elements can be treated as isoparametric elements and lead to zero strain under arbitrary rigid-body motion. Within the formulation several plate and beam finite elements were developed [17–19] that enable the analysis of structures subjected to large rotations and deformations. A two-dimensional shear deformable beam element has been introduced by Omar and Shabana [19]. This element uses a continuum mechanics approach to derive elastic forces can suffer from volumetric Poisson's locking, thickness locking and shear locking [20, 21]. The Poisson's locking can be avoided for thin beams by setting the Poisson ratio to zero, otherwise, the correction terms are needed as proposed by Sopanen and Mikkola [22]. As shown by Gerstmayr and Shabana [21] the combined thickness and shear locking can be avoided by introducing the additional shape function. Possible alternatives to eliminate locking phenomena are the redefied polynomial expansions with a reduced integration procedure [20] or order locking-free shear beam elements [23–25].Within ANCF it is also possible to implement the internal damping mechanisms based on continuum mechanics approach that dissipates the energy only when the system experiences some deformation [26]. As the ANCF formulation is relatively recent, it has received little attention regarding coupled thermo-structural problems. In [27] an ANCF formulation for the plate element is proposed that accounts for the aerothermoelastic behavior under thermal loading. For a simple Euler-Bernoulli beam the coupled thermo-structural analysis is presented in [28].

In this paper a new model of the bimetallic strip based on the ANCF formulation is presented. The individual strip of metal is modeled by a two-dimensional, shear-deformable beam element, originally proposed by Omar and Shabana [19] with the inclusion of the additional shape function to avoid the locking phenomena [21]. In order to simulate the dynamic response of bimetallic structures the formulation of the shear-deformable beam element [19] is extended to account for the thermally induced stresses. A uniform temperature field within the metal strip is proposed, whereas the thermal load is applied in the axial direction. The developed, coupled, thermo-structural, shear-deformable beam element made it possible to model the connectivity constraints at the interface between two adjacent strips and to predict the dynamic response under thermal loading. The dynamic response of the developed bimetallic strip model is compared with a general-purpose, finite-element software ANSYS using isoparametric brick elements. Finally, the applicability of the developed numerical model is demonstrated on a bimetallic strip subjected to high temperatures that cause large deformations and displacements to the structure.

This paper is organized as follows. In Section 2 the model of a bimetallic strip is presented together with the inclusion of thermal loading in the proposed beam element. Section 3 presents the verification and the applicability of the developed numerical model. Finally, the conclusions are drawn in Section 4.

2 Introduction of the thermal effect to the shear-deformable beam element

Bimetals are made of two strips of metals with different coefficients of thermal expansion that are bonded together. This difference enables the flat bimetallic strip to bend when heated up or cooled down. Here, the bimetallic strip is modeled as a system of planar shear-deformable beam elements [19] using the ANCF formulation. As the introduction of the thermal loading to the beam model is based on the continuum-mechanics approach, first the formulation of the shear-deformable beam element is presented.

Vector $\boldsymbol{r}$ that represents an arbitrary point p on the beam element (Fig. 1) can be written as:

$$\boldsymbol{r} = \mathbf{S}\boldsymbol{e}, \tag{1}$$

where $\mathbf{S}$ is the shape function of the shear-deformable beam element:

$$\mathbf{S} = \left[\begin{array}{ccccccc} s_1\mathbf{I} & s_2\mathbf{I} & s_3\mathbf{I} & s_4\mathbf{I} & s_5\mathbf{I} & s_6\mathbf{I} & s_7\mathbf{I} \end{array} \right], \tag{2}$$

The variable $\mathbf{I}$ represents the identity matrix of size 2x2 and the shape functions

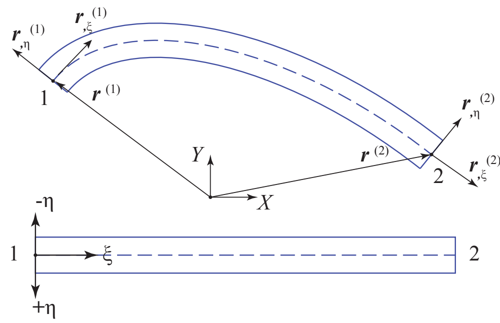

Figure 1: *Shear deformable beam element.*

s_i are defined as:

$$\begin{aligned} s_1 &= 1 - 3\alpha^2 + 2\alpha^3, \\ s_2 &= L(\alpha - 2\alpha^2 + \alpha^3), \\ s_3 &= H(1-\alpha^2)\beta, \\ s_4 &= 3\alpha^2 - 2\alpha^3, \\ s_5 &= L(-\alpha^2 + \alpha^3), \\ s_6 &= H\alpha^2\beta, \\ s_7 &= H\,L\beta(\alpha - \alpha^2), \end{aligned} \tag{3}$$

where $\alpha = \frac{x}{L}$, $\beta = \frac{y}{H}$, L is the element length, H is the element thickness and x, y are the element coordinates. In Eq. (1) the vector of the element nodal coordinates can be written as:

$$\boldsymbol{e} = \left[\begin{array}{ccccccc} \boldsymbol{r}^{\mathrm{T}}\big|_{x=0} & \boldsymbol{r}_x^{\mathrm{T}}\big|_{x=0} & \boldsymbol{r}_y^{\mathrm{T}}\big|_{x=0} & \boldsymbol{r}^{\mathrm{T}}\big|_{x=L} & \boldsymbol{r}_x^{\mathrm{T}}\big|_{x=L} & \boldsymbol{r}_y^{\mathrm{T}}\big|_{x=L} & \boldsymbol{r}_{yx}^{\mathrm{T}}\big|_{x=0} \end{array}\right]^{\mathrm{T}}, \tag{4}$$

where $\boldsymbol{r}^{\mathrm{T}}\big|_{x=0}$, $\boldsymbol{r}^{\mathrm{T}}\big|_{x=L}$ are the global displacements of the nodes and $\boldsymbol{r}_x^{\mathrm{T}}\big|_{x=0}$, $\boldsymbol{r}_y^{\mathrm{T}}\big|_{x=0}$, $\boldsymbol{r}_x^{\mathrm{T}}\big|_{x=L}$, $\boldsymbol{r}_y^{\mathrm{T}}\big|_{x=L}$ are the global slopes at the nodes and $\boldsymbol{r}_{yx}^{\mathrm{T}}\big|_{x=0}$ is the change over x of the gradient $\boldsymbol{r}_y^{\mathrm{T}}\big|_{x=0}$. The kinetic energy of the beam element is defined as follows:

$$T = \frac{1}{2}\int_V \rho \dot{\boldsymbol{r}}^{\mathrm{T}}\dot{\boldsymbol{r}}\mathrm{d}V = \frac{1}{2}\dot{\boldsymbol{e}}^{\mathrm{T}}\left(\int_V \rho \mathbf{S}^{\mathrm{T}}\mathbf{S}\mathrm{d}V\right)\dot{\boldsymbol{e}} = \frac{1}{2}\dot{\boldsymbol{e}}^{\mathrm{T}}\mathbf{M}\dot{\boldsymbol{e}}, \tag{5}$$

where $\mathbf{M}$ is a constant-mass matrix defined as:

$$\mathbf{M} = \int_V \rho \mathbf{S}^{\mathrm{T}}\mathbf{S}\mathrm{d}V. \tag{6}$$

The variable V is the element volume and ρ is the density of the beam material. The expression for the elastic forces is deduced according to the deformation gradient:

$$\mathbf{J} = \frac{\partial \boldsymbol{r}}{\partial x} = \begin{bmatrix} \frac{\partial r_1}{\partial x} & \frac{\partial r_1}{\partial y} \\ \frac{\partial r_2}{\partial x} & \frac{\partial r_2}{\partial y} \end{bmatrix} = \begin{bmatrix} \mathbf{S}_{1x}\boldsymbol{e} & \mathbf{S}_{1y}\boldsymbol{e} \\ \mathbf{S}_{2x}\boldsymbol{e} & \mathbf{S}_{2y}\boldsymbol{e} \end{bmatrix}, \tag{7}$$

where $\mathbf{S}_{\mathbf{i}x} = \frac{\partial \mathbf{S}_\mathbf{i}}{\partial x}$, $\mathbf{S}_{\mathbf{i}y} = \frac{\partial \mathbf{S}_\mathbf{i}}{\partial y}$ and $\mathbf{S}_\mathbf{i}$ is the i-th row of the element shape function. The Lagrangian strain tensor $\boldsymbol{\varepsilon}_\mathbf{m}$ can be written in the form:

$$\boldsymbol{\varepsilon}_\mathbf{m} = (\mathbf{J}^\mathrm{T}\mathbf{J} - \mathbf{I}) = \begin{bmatrix} \boldsymbol{e}^T\mathbf{S}_a\boldsymbol{e} - 1 & \boldsymbol{e}^T\mathbf{S}_c\boldsymbol{e} \\ \boldsymbol{e}^T\mathbf{S}_c\boldsymbol{e} & \boldsymbol{e}^T\mathbf{S}_b\boldsymbol{e} - 1 \end{bmatrix}, \tag{8}$$

where $\mathbf{I}$ is the identity matrix and the variables $\mathbf{S}_a$, $\mathbf{S}_b$ and $\mathbf{S}_c$ are defined as:

$$\mathbf{S}_a = \mathbf{S}_{\mathbf{1}x}^\mathrm{T}\mathbf{S}_{\mathbf{1}x} + \mathbf{S}_{\mathbf{2}x}^\mathrm{T}\mathbf{S}_{\mathbf{2}x}, \tag{9}$$

$$\mathbf{S}_b = \mathbf{S}_{\mathbf{1}y}^\mathrm{T}\mathbf{S}_{\mathbf{1}y} + \mathbf{S}_{\mathbf{2}y}^\mathrm{T}\mathbf{S}_{\mathbf{2}y}, \tag{10}$$

$$\mathbf{S}_c = \mathbf{S}_{\mathbf{1}x}^\mathrm{T}\mathbf{S}_{\mathbf{1}y} + \mathbf{S}_{\mathbf{2}x}^\mathrm{T}\mathbf{S}_{\mathbf{2}y}. \tag{11}$$

The strain tensor is symmetrical and can be written as:

$$\boldsymbol{\varepsilon} = \begin{bmatrix} \varepsilon_1 & \varepsilon_2 & \varepsilon_3 \end{bmatrix}^\mathrm{T}, \tag{12}$$

where the components of the strain vector are:

$$\varepsilon_1 = \frac{1}{2}(\boldsymbol{e}^\mathrm{T}\mathbf{S}_\mathbf{a}\boldsymbol{e} - 1), \tag{13}$$

$$\varepsilon_2 = \frac{1}{2}(\boldsymbol{e}^\mathrm{T}\mathbf{S}_\mathbf{b}\boldsymbol{e} - 1), \tag{14}$$

$$\varepsilon_3 = \frac{1}{2}(\boldsymbol{e}^\mathrm{T}\mathbf{S}_\mathbf{c}\boldsymbol{e}). \tag{15}$$

The general expression for the strain energy is written using the strain vector $\boldsymbol{\varepsilon}$ and the stress vector $\boldsymbol{\sigma}$ as:

$$\boldsymbol{\sigma} = \begin{bmatrix} \sigma_1 & \sigma_2 & \sigma_3 \end{bmatrix}^\mathrm{T}, \tag{16}$$

$$U = \frac{1}{2}\int_V \boldsymbol{\sigma}^\mathrm{T}\boldsymbol{\varepsilon}\,\mathrm{d}V. \tag{17}$$

Using the constitutive equations, the relation between stress and strain can be obtained:

$$\boldsymbol{\sigma} = \mathbf{E}\boldsymbol{\varepsilon}, \tag{18}$$

where $\mathbf{E}$ is the matrix of the elastic constants of the material. For an isotropic, homogeneous material, the matrix $\mathbf{E}$ can be expressed in terms of Lame's constants λ and μ:

$$\mathbf{E} = \begin{bmatrix} \lambda + 2\mu & \lambda & 0 \\ \lambda & \lambda + 2\mu & 0 \\ 0 & 0 & 2\mu \end{bmatrix}. \tag{19}$$

Using Eqs. (18) and (19), the strain energy can be rewritten as:

$$U = \frac{1}{2}\int_V \boldsymbol{\varepsilon}^\mathrm{T}\mathbf{E}\boldsymbol{\varepsilon}\,\mathrm{d}V. \tag{20}$$

The vector of the elastic forces $\boldsymbol{Q_e}$ is deduced using the strain energy U:

$$\boldsymbol{Q}_e^{\mathrm{T}} = \frac{\partial U}{\partial \boldsymbol{e}} = \boldsymbol{e}^{\mathrm{T}}\mathbf{K}. \tag{21}$$

The variable $\mathbf{K}$ presents the stiffness matrix:

$$\mathbf{K} = (\lambda + 2\mu)\mathbf{K_1} + \lambda\mathbf{K_2} + 2\mu\mathbf{K_3}, \tag{22}$$

where its sub-parts are defined as:

$$\mathbf{K_1} = \frac{1}{4}\int_V \left(\mathbf{S}_{a1}(\boldsymbol{e}^{\mathrm{T}}\mathbf{S}_a\boldsymbol{e} - 1) + \mathbf{S}_{b1}(\boldsymbol{e}^{\mathrm{T}}\mathbf{S}_b\boldsymbol{e} - 1)\right)\,\mathrm{d}V, \tag{23}$$

$$\mathbf{K_2} = \frac{1}{4}\int_V \left(\mathbf{S}_{a1}(\boldsymbol{e}^{\mathrm{T}}\mathbf{S}_b\boldsymbol{e} - 1) + \mathbf{S}_{b1}(\boldsymbol{e}^{\mathrm{T}}\mathbf{S}_a\boldsymbol{e} - 1)\right)\,\mathrm{d}V, \tag{24}$$

$$\mathbf{K_3} = \frac{1}{4}\int_V \left(\mathbf{S}_{c1}(\boldsymbol{e}^{\mathrm{T}}\mathbf{S}_c\boldsymbol{e} - 1)\right)\,\mathrm{d}V \tag{25}$$

and

$$\begin{aligned} \mathbf{S}_{a1} &= \mathbf{S}_a + \mathbf{S}_a^{\mathrm{T}}, \\ \mathbf{S}_{b1} &= \mathbf{S}_b + \mathbf{S}_b^{\mathrm{T}}, \\ \mathbf{S}_{c1} &= \mathbf{S}_c + \mathbf{S}_c^{\mathrm{T}}. \end{aligned} \tag{26}$$

Finally, the equation of motion for the beam element can be written as:

$$\mathbf{M}\ddot{e} + \boldsymbol{Q}_e = \boldsymbol{Q}_{ext}, \tag{27}$$

where $\boldsymbol{Q}_{ext}$ is the vector of generalized external forces and $\boldsymbol{Q}_e$ is the vector of elastic forces given by:

$$\boldsymbol{Q}_e = \mathbf{K}\boldsymbol{e} \tag{28}$$

The inclusion of the thermal effect in the shear-deformable beam element has not yet been presented in the literature; therefore, a detailed formulation is given. It is assumed that the temperature field along the beam element is homogeneous. This can be considered for the majority of bimetallic strips where the temperature field is the result of the differential current passing through the element. The change of the temperature within the element is in direct correlation with the deformations. As the bending deformation of the bimetallic strip is mainly governed by the axial strain, the thermal load is only applied in this direction. Therefore, the strain vector due to the thermal load can be written as:

$$\boldsymbol{\varepsilon}_{\mathrm{T}} = \begin{bmatrix} \Delta T\alpha_T & 0 & 0 \end{bmatrix}^{\mathrm{T}}. \tag{29}$$

Here, ΔT is the change in the temperature field and α_T is the coefficient of thermal expansion. By using Eq. (29) in Eq. (18) it is possible to rewrite the relation between the stress and the strain as:

$$\boldsymbol{\sigma} = \mathbf{E}\left(\boldsymbol{\varepsilon} - \boldsymbol{\varepsilon}_T\right), \tag{30}$$

Considering Eq. (30) and Eqs. (18)-(21), it is possible to deduce the parts of the stiffness matrix $\mathbf{K}_1$ and $\mathbf{K}_2$ that account for the thermal load in the axial direction:

$$\mathbf{K_1} = \frac{1}{4}\int_V \left[\mathbf{S}_{a1}(\mathbf{e}^{\mathrm{T}}\mathbf{S}_a\mathbf{e} - 2\,\Delta T\alpha_T - 1) + \mathbf{S_{b1}}(\boldsymbol{e}^{\mathrm{T}}\mathbf{S_b}\boldsymbol{e} - 1)\right]\,\mathrm{d}V, \tag{31}$$

$$\mathbf{K_2} = \frac{1}{4}\int_V \left[\mathbf{S_{a1}}(\boldsymbol{e}^{\mathrm{T}}\mathbf{S_b}\boldsymbol{e} - 1) + \mathbf{S_{b1}}(\boldsymbol{e}^{\mathrm{T}}\mathbf{S_a}\boldsymbol{e} - 2\,\Delta T\alpha_T - 1)\right]\,\mathrm{d}V. \tag{32}$$

The part of the stiffness matrix $\mathbf{K}_3$ remains the same and is given by Eq. (25). Using the proposed procedure it is possible to introduce the thermal loading into the shear-deformable beam element, which is essential to represent the bimetallic effect. The resulting stiffness matrix is highly non-linear with complex and extensive expressions that define its elements.

3 Formulation of the bimetallic-strip model

The model of the bimetallic strip is based on the thermo-structural, shear-deformable beam element by introducing the connectivity constraint between two adjacent beam elements (Fig. 2). The equality of displacement is proposed at the location of the connection nodes in order to represent the line contact between two strips of metal. The constraint equations can be written as:

$$\mathbf{C}_1 = \mathbf{r}^i(\xi = 0, \eta = 0.5) - \mathbf{r}^j(\xi = 0, \eta = -0.5) \tag{33}$$

$$\mathbf{C}_2 = \mathbf{r}^i(\xi = 1, \eta = 0.5) - \mathbf{r}^j(\xi = 1, \eta = -0.5) \tag{34}$$

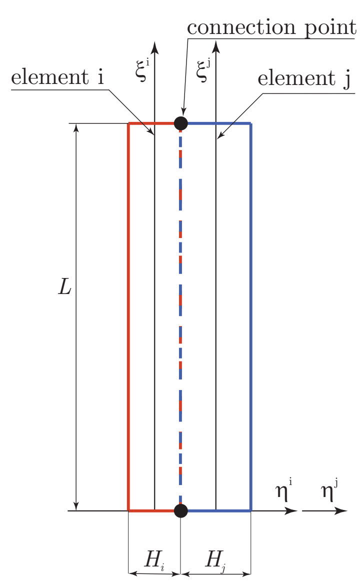

Figure 2: *Connection points between two beam elements.*

As usual, the discretization of the bimetallic strip is performed along its length, while the connectivity constraints between the two flexible beam elements must be introduced as presented in Fig. 3. First, the equality of the displacement must be considered:

$$\mathbf{C}_3 = \mathbf{r}^i(\xi = 1, \eta = 0) - \mathbf{r}^{i+1}(\xi = 0, \eta = 0), \tag{35}$$

$$\mathbf{C}_4 = \mathbf{r}^j(\xi = 1, \eta = 0) - \mathbf{r}^{j+1}(\xi = 0, \eta = 0) \tag{36}$$

and, secondly, the equality of rotation with respect to the ξ and η coordinates:

$$\mathbf{C}_5 = \frac{\partial}{\partial \xi}\mathbf{r}^i(\xi = 1, \eta = 0) - \frac{\partial}{\partial \xi}\mathbf{r}^{i+1}(\xi = 0, \eta = 0,) \tag{37}$$

$$\mathbf{C}_6 = \frac{\partial}{\partial \xi}\mathbf{r}^j(\xi = 1, \eta = 0) - \frac{\partial}{\partial \xi}\mathbf{r}^{j+1}(\xi = 0, \eta = 0), \tag{38}$$

$$\mathbf{C}_7 = \frac{\partial}{\partial \eta}\mathbf{r}^i(\xi = 1, \eta = 0) - \frac{\partial}{\partial \eta}\mathbf{r}^{i+1}(\xi = 0, \eta = 0), \tag{39}$$

$$\mathbf{C}_8 = \frac{\partial}{\partial \eta}\mathbf{r}^j(\xi = 1, \eta = 0) - \frac{\partial}{\partial \eta}\mathbf{r}^{j+1}(\xi = 0, \eta = 0). \tag{40}$$

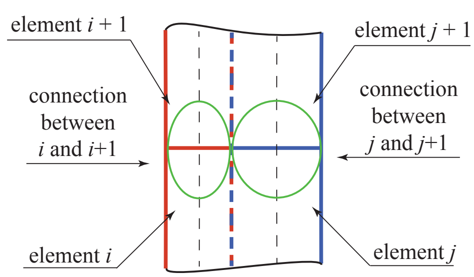

Figure 3: *Connectivity constraints along the length of the bimetallic strip segment.*

The presented connectivity constraints enable the representation of the bimetallic-strip model using flexible bodies. Along the thickness of the bimetallic strip the connectivity between the adjacent beam elements i and j is proposed at the element nodal coordinates ($\xi = 0$, $\xi = 1$). Note that it would be possible to introduce additional connectivity nodes along the beam elements in order to more realistically represent the welded bonding line contact between the two metallic strips. However, the application of additional connectivity nodes along the beam length would require higher-order element functions, as otherwise a numerically induced stiffness is introduced to the system. Although the connectivity constraints are applied only at the element nodal points, a relatively good convergence of the proposed bimetallic-strip model can be observed, as shown

in section 4.
The equations of motion for the beam element can be written as:

$$\mathbf{M}^j\,\ddot{\mathbf{e}}^j + \underbrace{\mathbf{K}\mathbf{e}}_{-\mathbf{Q}_f^j} = \mathbf{Q}_e^j. \tag{41}$$

The system of equations of motion, including all the beam elements in the bimetallic strip and the constraint equations describing the connectivity constraint, finally has the shape:

$$\begin{bmatrix} \mathbf{M} & \mathbf{C}_e^{\mathrm{T}} \\ \mathbf{C}_e & \mathbf{0} \end{bmatrix} \begin{Bmatrix} \ddot{\mathbf{e}} \\ \boldsymbol{\lambda} \end{Bmatrix} = \begin{bmatrix} \mathbf{Q}_f + \mathbf{Q}_e \\ \mathbf{Q}_d \end{bmatrix}, \tag{42}$$

where $\mathbf{M}$ is the constant-mass matrix, $\mathbf{C}_e$ is the Jacobian of the constraint equations and $\boldsymbol{\lambda}$ is the vector of Lagrange multipliers. The vector $\mathbf{Q}_e$ is the generalized force vector that includes external forces, $\mathbf{Q}_f$ is the generalized force due to the stiffness, and $\mathbf{Q}_d$ is obtained through differentiation of the constraints:

$$\mathbf{Q}_d = -\frac{\partial\left(\mathbf{C_e}\dot{\mathbf{e}}\right)}{\partial \mathbf{e}}\dot{\mathbf{e}}. \tag{43}$$

The presented formulation can be extended to three-dimensional analysis by using 3D shear deformable beam elements as they are presented in [21, 29]. This would require the redefinition of constraint equations by introducing an additional connectivity constraint between adjacent element in the z direction. However the strain vector given by Eq. (29) would remain the same.

4 Verification of the bimetallic-strip numerical model

In this section a bimetallic strip clamped on one side and subjected to thermal loading is considered (Fig. 4a). The simulations were performed proposing a standard bimetallic strip TB177 (DIN 1715) with the material properties defined in Table 1.

First, the mesh-convergence analysis is performed in order to assess the convergence of the solution with respect to the mesh refinement. The influence of the number of elements is determined by computing the displacement error at the free end of the strip (point A) with respect to the reference model with 20 elements.

$$err = \frac{1}{N}\sum_{i=1}^{N}\frac{x_i - x_{i,\,20\mathrm{elem}}}{x_{i,\,20\mathrm{elem}}} \tag{44}$$

The simulations are performed in the time interval $t \in [0, 0.005]\,$s where the strip segment is uniformly exposed to the temperature profile presented in Fig. 4b with a maximum temperature of 200°C. It is clear (Fig. 5) that the error decreases exponentially with respect to the number of elements. Due to the

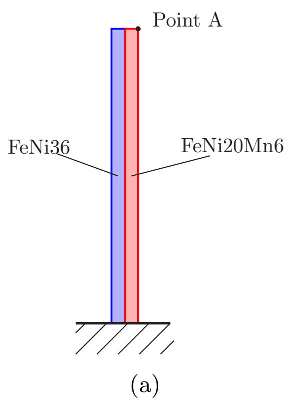

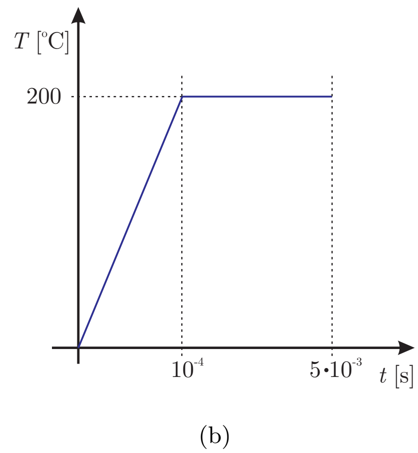

Figure 4: Numerical simulation of bimetallic strip; a) Numerical model; b) Temperature profile.

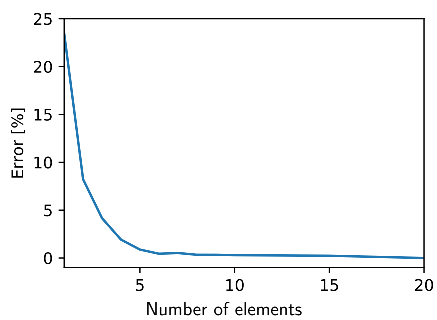

Figure 5: The error of the point A displacement versus the number of elements.

high-order shape function a relatively small number of elements can provide high accuracy of the solution. Consequently, all the forgoing simulations will be performed using a discretization with 20 beam elements. The verification study was conducted by comparing the displacement response with a general-purpose, finite-element software ANSYS. The reference finite-element model was meshed with SOLID186 brick elements. The contact between the strips of metal was modeled using TARGE170 and CONTA173 elements. The transient structural analysis was conducted by considering large deflections and rotations. Hence, the rigid-body effect (e.g., large rotation) is taken into account; however, the strains are assumed to be small. The comparison of the responses at point A between the developed ANCF model and the ANSYS finite-element model are presented in Fig. 6. Good agreement between the two models confirms the adequacy of the proposed bimetallic-strip model using the ANCF-coupled,

Table 1: The bimetallic strip TB 1577 (DIN 1715) material and geometric parameters.

Parameter	Symbol	Value
Passive component	1	FeNi36 (invar)
Active component	2	FeNi20Mn6
Length	l_1, l_2	0.034 m
Width	w_1, w_2	0.005 m
Thickness	t_1, t_2	0.0005 m
Density	ρ_1	7750 kg/m^3
	ρ_2	8055 kg/m^3
Young's Modulus	E_1	200 MPa
	E_2	145 MPa
Poisson's ratio	μ_1	0
	μ_2	0
Thermal expansion coefficient	α_1	2.85 $\times$ 10e^{-5} K^{-1}
	α_2	1.2 $\times$ 10e^{-6} K^{-1}

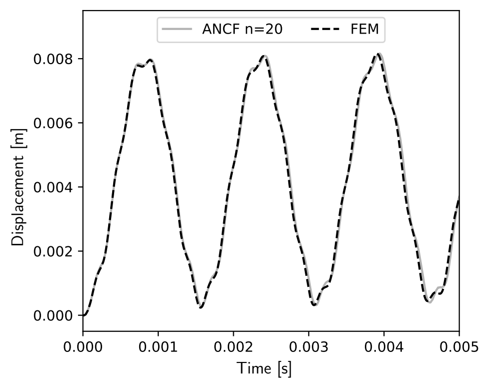

Figure 6: Comparison of displacements at point A.

thermo-structural formulation. Moreover, the comparison of the full-field displacements along the strip length (Fig. 7) additionally demonstrates the validity of the developed bimetallic-strip model. In order to show the applicability of the developed numerical model of the bimetallic strip (ANFC formulation), the system is exposed to a temperature profile (Fig. 4b) with an increased maximum temperature $T_{max} = 600°$C. The resulting displacement for three different time points is presented in Fig. 8. In this case the beam elements are exposed to large deflections and deformations. Moreover, the rigid-body motions and the large rotations have a significant influence on the system's dynamic response.

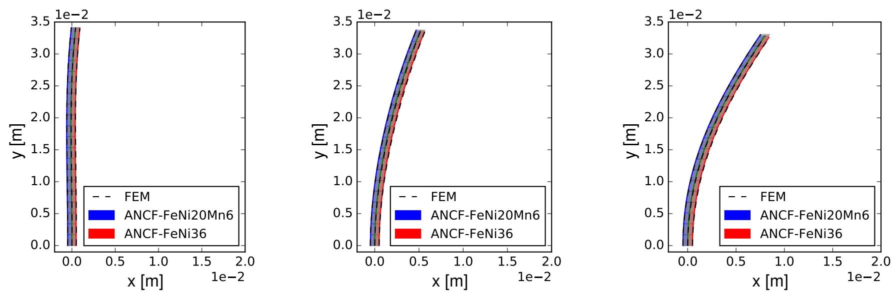

(a) (b) (c)

Figure 7: Comparison of displacements of the bimetallic strip ($T_{max} = 200°$C); a) $t = 1 \cdot 10^{-4}$ s, b) $t = 5 \cdot 10^{-4}$ s, c) $t = 9 \cdot 10^{-4}$ s.

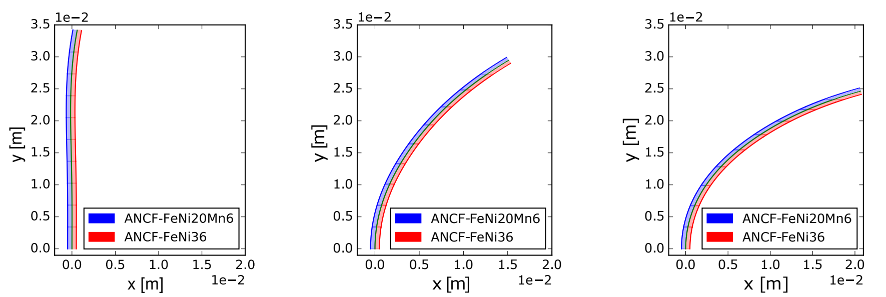

(a) (b) (c)

Figure 8: Displacement of bimetallic strip ($T_{max} = 600°$C); a) $t = 1 \cdot 10^{-4}$ s, b) $t = 5 \cdot 10^{-4}$ s, c) $t = 9 \cdot 10^{-4}$ s.

5 Summary and conclusions

In this paper a new model for a bimetallic strip based on the ANCF formulation is presented. The basic model of a shear-deformable beam element was extended in order to account for the thermally induced stresses in the axial direction. Considering a uniform temperature distribution along the beam element, a derivation of the stiffness matrix is presented that accounts for the thermal loading. A numerical verification of the proposed model is performed by showing the convergence of the solution. The verification study was conducted by comparing results with a general-purpose, finite-element software where classic isoparametric brick elements were used. It was demonstrated that a relatively small number of high-order beam elements can effectively predict the dynamic response of bimetallic structures. Moreover, using the proposed coupled thermo-structural formulation the beams in the bimetallic-strip model can be treated as isoparametric elements. Therefore, the presented formulation of the bimetallic element results in zero strains under arbitrary rigid-body motion and enables

an exact modeling of the rigid-body inertia, which is not the case when using the classic beam finite-element formulation.
The presented approach to model bimetallic structures can be applied also to model general composite structures. In order to properly present such structures also the adhesive between layers should be modeled as a layer with properly defined material properties.

References

[1] M. Sedighi, B. N. Dardashti, A review of thermal and mechanical analysis in single and bi-layer plate, Materials Physics and Mechanics 14 (1) (2012) 37–46.

[2] S. Boisseau, G. Despesse, S. Monfray, O. Puscasu, T. Skotnicki, A bimetal and electret-based converter for thermal energy harvesting, ArXiv e-prints (2012) 1–3.

[3] Y. S. Muzychka, M. M. Yovanovich, Analytic models to compute transient thermal stresses in bimaterial systems, in: Advanced Technology for Electronic Packaging, Austin, TX, 1996.

[4] W.-H. Chu, M. Mehregany, R. L. Mullen, Analysis of tip deflection and force of a bimetallic cantilever microactuator, Journal of Micromechanics and Microengineering 3 (1) (1993) 4–7.

[5] D. S. Ross, A. Cabal, D. Trauernicht, J. Lebens, Temperature-dependent vibrations of bilayer microbeams, Sensors and Actuators A: Physical 119 (2) (2005) 537–543.

[6] W. Suocheng, H. Yongping, L. Shuangjie, The design and analysis of a MEMS electrothermal actuator, Journal of Semiconductors 36 (4) (2015) 1–5.

[7] Q. Zou, U. Sridhar, R. Lin, A study on micromachined bimetallic actuation, Sensors and Actuators A: Physical 78 (2) (1999) 212–219.

[8] S. Timoshenko, Analysis of Bimetal Thermostats, Journal of the Optical Society of America 11 (1925) 233–255.

[9] A. Mirman B. Interlaminar Stresses in Layered Beams, Journal of Electronic Packaging 114 (1992) 389–396.

[10] E. Suhir, Interfacial Stresses in Bimetal Thermostats, Journal of Applied Mechanics 56 (1989) 595–560.

[11] E. Suhir, Thermally Induced Interfacial Stresses in Elongated Bimaterial Plates, Applied Mechanics Reviews 42 (1989) 252–262.

[12] T.-R. Hsu, MEMS and microsystems : design, manufacture, and nanoscale engineering, 2nd Edition, John Wiley & Sons, Inc., New Jersey, 2008.

[13] A. Shabana, A., Dynamics of Multibody Systems, 3rd Edition, Cambridge University Press, 2005.

[14] A. A. Shabana, Computer implementation of the absolute nodal coordinate formulation for flexible multibody dynamics, Nonlinear Dynamics 16 (3) (1998) 293–306.

[15] J. L. Escalona, H. A. Hussien, A. A. Shabana, Application of the absolute nodal co-ordinate formulation to multibody system dynamics, Journal of Sound and Vibration 214 (1998) 833–851.

[16] G. Čepon, M. Boltežar, Dynamics of a belt-drive system using a linear complementarity problem for the belt–pulley contact description, Journal of Sound and Vibration 319 (3) (2009) 1019–1035.

[17] A. M. Mikkola, A. A. Shabana, A new plate element based on the absolute nodal coordinate formulation, ASME Design Engineering Technical Conferences and Computers and Information in Engineering Conference, Pittsburgh, PA, September (2001) 9–12.

[18] K. E. Dufva, J. T. Sopanen, A. M. Mikkola, A two-dimensional shear deformable beam element based on the absolute nodal coordinate formulation, Journal of Sound and Vibration 280 (2005) 719–738.

[19] M. A. Omar, A. A. Shabana, A two-dimensional shear deformable beam for large rotation and deformation problems, Journal of Sound and Vibration 243 (3) (2001) 565–576.

[20] D. G. Vallejo, A. M. Mikkola, J. L. Escalona, A new locking-free shear deformable finite element based on absolute nodal coordinates, Nonlinear Dynamics 50 (2007) 249–264.

[21] J. Gerstmayr, A. A. Shabana, Analysis of Thin Beams and Cables Using the Absolute Nodal Co-ordinate Fromulation, Nonlinear Dynamics 45 (2006) 109–130.

[22] J. T. Sopanen, A. M. Mikkola, Description of Elastic Forces in Absolute Nodal Coordinate Formulation, Nonlinear Dynamics 34 (2003) 53–74.

[23] M. K. Matikainen, O. N. Dmitrochenko, M. A. M., Beam elements with trapezoidal cross section deformation modes based on absolute nodal coordinate formulation, Procedings of the International Conference of Numerical Analysis and Applied MAthematics, Rhodes, Greece.

[24] J. Gerstmayr, H. Irschik, On the correct representation of bending and axial deformation in the absolute nodal coordinate formulation with an elastic line approach., Journal of Sound and Vibration 318 (2008) 461–487.

[25] K. E. Dufva, J. T. Sopanen, M. A. M., A two-dimensional shear deformable beam element based on the absolute nodal coordinate formulation, Journal of Sound and Vibration 280 (2005) 719–738.

[26] D. G. Vallejo, J. Valverde, J. Dominguez, An Internal Damping Model for the Absolute Nodal Coordinate Formulation, Nonlinear Dynamics 42 (2005) 347–369.

[27] L. K. Abbas, X. Rui, P. Marzocca, Aerothermoelastic analysis of panel flutter based on the absolute nodal coordinate formulation, Multibody System Dynamics 33 (2) (2015) 163–178.

[28] Z. Shen, Q. Tian, X. Liu, G. Hu, Thermally induced vibrations of flexible beams using Absolute Nodal Coordinate Formulation, Aerospace Science and Technology 29 (1) (2013) 386–393.

[29] A. A. Shabana, R. Y. Yakoub, Three dimensional absolute nodal coordinate formulation for beam elements: Theory, Journal of Mechanical Design 123 (3) (2001) 606–613.